ADVANCED ENERGY MATERIALS
www.advenergymat.de

Role of Transition Metal in Fast Oxidation Reaction on the Pt_3TM (111) (TM = Ni, Co) Surfaces

Yong Su Kim, Sang Ho Jeon, Aaron Bostwick, Eli Rotenberg, Philip N. Ross, Vojislav R. Stamenkovic, Nenad M. Markovic, Tae Won Noh, Seungwu Han, and Bongjin Simon Mun**

The fundamental bonding interactions between oxygen and metal surfaces play an important role in understanding commercially important catalytic reactions.[1] The subtle changes of bonding mechanism on the metal surfaces can make a critical difference in the electrochemical activity. Pt and Pt-alloys, one of the most extensively investigated catalyst systems, are remarkable catalysts in transforming the chemical state of oxygen in a variety of molecules, i.e., oxidation converter for CO[2–4] and NO_X[5–7] and as uniquely active electrode materials for both cathode and anode in fuel cells.[8–10] However, the realization of commercially viable fuel cells for transportation requires significantly lower Pt content and better reaction kinetics. Recent investigations on the Pt-based alloys found that adding transition metal (TM) resulted in higher catalytic activity[11–14] and suggested that modified electronic structure of Pt-TM system could be a source of its improved catalytic reactions.

Prof. Y. S. Kim,[†] Dr. A. Bostwick, Dr. E. Rotenberg
Advanced Light Source
Lawrence Berkeley National Laboratory
Berkeley, California 94720 USA
Dr. S. H. Jeon,[†] Prof. S. Han
Department of Materials Science & Engineering
Research Institute of Advanced Materials
Seoul National University
Seoul 151-744 Korea
E-mail: hansw@snu.ac.kr
Dr. P. N. Ross
Material & Molecular Research Division
Lawrence Berkeley National Laboratory
Berkeley, California 94720 USA
Dr. V. R. Stamenkovic, Dr. N. M. Markovic
Material Science Division
Argonne National Laboratory
Argonne, Illinois 60439 USA
Prof. Y. S. Kim, Prof. T. W. Noh
CFI-CES, IBS and Department of Physics & Astronomy
Seoul National University
Seoul 151-747 Korea
Prof. B. S. Mun
Department of Physics & Photon Science
School of Physics & Chemistry
Ertl Center for Electrochemistry and Catalyst
Gwangju Institute of Science and Technology
Gwangju 500-712 Korea
E-mail: bsmun@gist.ac.kr
[†] Y.S.K. and S.H.J. contributed equally to this work

DOI: 10.1002/aenm.201300166

In explaining trends in catalytic activity of Pt-TM alloys, the *d*-band electronic model has been proposed. According to this model,[15] the chemical bonding of adsorbates on the metal surfaces is closely related to a feature in the total density of states (DOS), i.e. average location of DOS contributed by *d* electrons (so called *d*-band center) near the Fermi level.[14,16,17] From a molecular orbital point of view, modification of the oxygen-metal bonding comes from changes in the coupling strength between oxygen 2*p* and metal *d* states.[17] That is, the modified surface structure, i.e., Pt top-surface/TM sub-surface, alters the surface electronic structure and hence changes the coverage of all oxygen-containing species at a given electrode potential. The change of adsorption properties by so-called spectator species through the electronic modification produces the enhanced catalytic activity of the Pt-alloy catalyst.

The total DOS is readily accessible from the normal X-ray photoemission spectroscopy (XPS). However, for the present purposes, it is essential to obtain the energy-and-momentum resolved near-surface band structure. Such measurements are enabled by angle-resolved XPS (ARPES), but few experimental observations have been performed for bimetallic systems. Therefore, a deep understanding of (1) the role of TM in altering the surface electronic structure of Pt and (2) the correlation between the surface electronic structure and bonding with oxygen-containing species is yet to be obtained.

Here, we report a direct visualization of surface electronic band structure with high performance ARPES, allowing us to investigate the bonding interaction between chemically adsorbed atomic oxygen and Pt_3TM(111) (TM = Ni and Co) surfaces, which is known as one of the most-active catalytic bimetallic surfaces for oxygen chemisorption and reduction process. It is found that the *d*-electrons of subsurface TM do not contribute to direct chemical bonding with oxygen. Supported by density functional theory (DFT) calculations, we show that the main origin of the weakened Pt-O bonding is due to the suppression of Pt surface-states near the Fermi level, which is a result of the change in interlayer potential, i.e. charge polarization, between Pt-top and TM-subsurface. Our results highlight the critical role of the sub-surface TM in modifying the electronic structure of the Pt surface layer that in turn tunes the surface chemical reactivity.

The chemical states of oxygen on the Pt_3TM(111) surfaces are characterized with the Pt 4*f* and O 1*s* core level spectra as a function of temperature, showing transition from a molecularly to chemically bonded state. On the clean surface of Pt(111) and Pt_3TM(111) (see Supporting

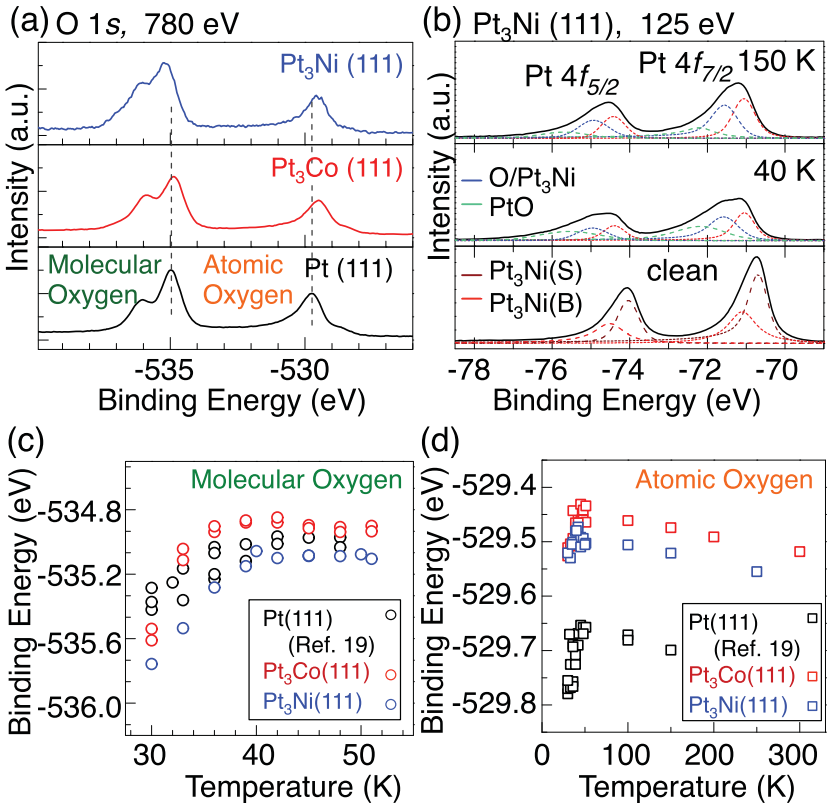

Figure 1. a) Core level spectra of O 1*s* of Pt, Pt_3Co, and $Pt_3Ni(111)$ measured at 30 K with 780 eV. Molecularly adsorbed (physisorbed) and atomically adsorbed (chemisorbed) oxygen are labeled. b) Pt 4*f* core level spectra of $Pt_3Ni(111)$ at 125 eV. The spectral feature of bulk-related, surface-related, chemisorbed atomic oxygen, and PtO-component are represented by $Pt_3Ni(B)$ (red), $Pt_3Ni(S)$ (dark red), O/Pt_3Ni (blue), and PtO (green), respectively. c,d) Temperature dependence of binding energy of physisorbed oxygen molecule and chemisorbed oxygen atom in the range of 30 – 51 K. The O/Pt(111) data were obtained from Ref. [19].

information, Figure S1), oxygen molecules were dosed at 30 K. As shown in **Figure 1**a, oxygen molecules are adsorbed with van der Waals interaction on the $Pt_3TM(111)$ surfaces, i.e., the physisorbed state, at low temperature (T < 40 K). Then, conversion into a chemisorbed state occurs at around 40 K.[18] During this thermally activated transition process, molecular oxygen dissociates into chemisorbed atomic oxygen[19] (O/Pt_3TM). A surface oxide (PtO) is also formed as by-product and was discussed previously.[19] Another important feature in Figure 1b is that surface-component of Pt 4*f* (i.e., $Pt_3Ni(S)$) from Pt-skin layer on the $Pt_3Ni(111)$ is located at the higher binding energy (–70.70 eV) compared to that of the Pt 4*f* (–70.54 eV)[19] (not shown here) on the clean Pt(111). This variation of 0.15 eV reflects the characteristic of charge state of the Pt top-surface layer on $Pt_3Ni(111)$, which is distinct from that of Pt(111). The discussion of the charge-distribution on Pt3TM, i.e., charge polarization, between surface and surface-subsurface layer will be given later.

The O 1*s* core level spectra of the physisorbed molecular oxygen on the Pt,[19] Pt_3Ni, and $Pt_3Co(111)$ surfaces, displayed in Figure 1c, reflects the behavior of the Pt 4*f* as the function of temperature. As is well known, the oxygen molecules in a physisorption state do not form chemical bonds with the metal surface. The interaction can be explained in terms of a potential energy surface.[20,21] Therefore, physisorbed oxygen molecules should experience nearly the same surface potential regardless of atom types in the subsurface layer. As shown in Figure 1c, the binding energies of O 1*s* for the physisorbed state follow similar behavior in all three surfaces; this indicates the surface layers of $Pt_3TM(111)$ are covered only with Pt atoms. In addition, core level spectra of Co 2*p* and Ni 2*p* from Pt_3TM do not exhibit any variation regardless of whether oxygen is chemisorbed on the surface or not, which again indicates the formation of Pt-skin layer on the surface (see Supporting information, Figure S2). Interestingly, the O 1*s* spectra for the chemisorbed atomic oxygen show significant changes as substrate varies, as displayed in Figure 1a. The binding energy of chemisorbed atomic oxygen on Pt(111)[19] is clearly higher than that on Pt_3Ni and $Pt_3Co(111)$ (Figure 1d).

To investigate the details of the bonding interaction between Pt surface atom and chemisorbed atomic oxygen on the $Pt_3TM(111)$ surfaces, we obtained a constant energy map at the Fermi level, E_F, and valence band structure in the first Brillouin zone by performing ARPES measurements. Here, we present only results from $Pt_3Ni(111)$ as representative of general features for all the $Pt_3TM(111)$ surfaces. As presented in **Figure 2**a and Figure 2b, the Fermi surfaces of clean $Pt_3Ni(111)$ undergo little change even after chemical bonding with atomic oxygen. Figure 2c and Figure 2d show a band structure cut along the ΓKM direction for clean $Pt_3Ni(111)$ and $O/Pt_3Ni(111)$. For clear comparison, the cuts of the clean surface band (filled circles) and that of oxygen-adsorbed one (empty squares) are plotted together in Figure 2e, which verify again that no significant change occurs after chemical bonding with atomic oxygen. This interesting result indicates a weak hybridization (i.e., nearly neutral charge-transfer) between oxygen and surface Pt atom. Another significant point to be noted is that $Pt_3Ni(111)$ show much less surface-state density than Pt(111)[22] near the Fermi level. The surface-state, which is localized at the surface layer, was previously identified as the key component in chemical bonding interaction in oxidation mechanism of the Pt(111) surface.[22] Especially, one surface-state near M symmetry point, which has $d_{xz,yz}$ character, was shown to contribute to weak hybridization with chemisorbed atomic oxygen, accompanied by minimal charge-transfer.[22] In the present work, we carefully identified surface-states of $Pt_3Ni(111)$ by observing little dispersion of spectral function along momentum axis, $k_\perp$, perpendicular to the surface (see Supporting information, Figure S3) and reconfirmed the less identified surface-states near the Fermi level. In addition, as displayed in Figure 2, there is no discernible band shift at the symmetry points including M point, indicating no considerable charge-transfer event was taking place.

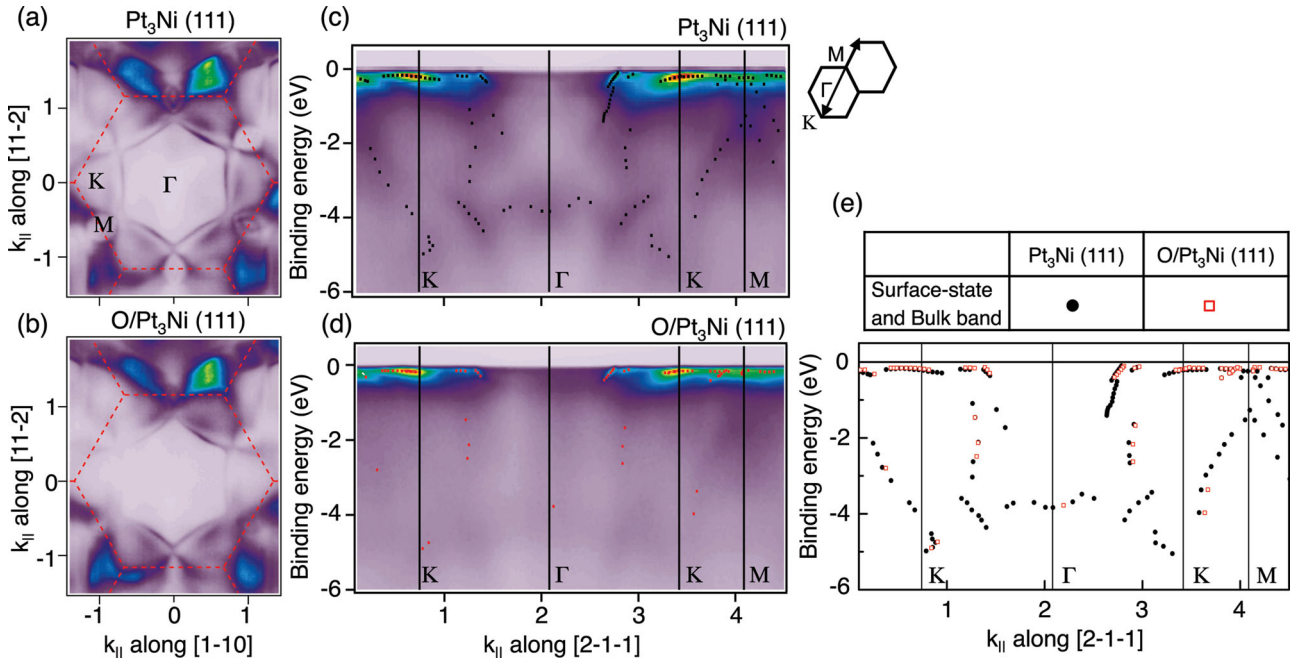

Figure 2. a,b) Constant-energy maps at the Fermi level (E_F) for the clean Pt_3Ni and $O/Pt_3Ni(111)$ surface. Red dashed line denotes the Brillouin zone boundary. c,d) Experimental energy band of clean Pt_3Ni and O/Pt_3Ni (111) along $\bar{\Gamma}\bar{M}$ direction. Black circle and red square are guidelines of the band dispersion for the clean crystal surfaces and surface covered with chemisorbed atomic oxygen, respectively. e) Surface band structure for the Pt_3Ni and $O/Pt_3Ni(111)$.

To clarify the specific role of TM in bonding interaction with chemisorbed atomic oxygen, we performed DFT calculations using the VASP code.[23,24] To model the Pt-TM(111), we used a slab consisting of 15 Pt(111) layers and inserted ~14 Å of vacuum between periodic images. Then, we substituted two Pt atoms at both sub-surface layers with TM atoms. Total energy and band structure calculations with spin polarization were carried out for Pt(111), O(fcc-hollow site)/Pt(111), Pt-TM(111), and O(fcc-hollow site)/Pt-TM(111). The adsorption energy of oxygen on the Pt-TM(111) relative to that of oxygen on the Pt(111) was calculated as follows:

$$\Delta E_{ad} = \left[E_{tot}^{O/\,Pt-TM} - E_{tot}^{Pt-TM}\right] - \left[E_{tot}^{O/\,Pt} - E_{tot}^{Pt}\right] \quad (1)$$

where $E_{tot}^{O/\,Pt-TM}$, E_{tot}^{Pt-TM}, $E_{tot}^{O/\,Pt}$, and E_{tot}^{Pt} indicate the total energies of the O/Pt-TM(111), Pt-TM(111), O/Pt(111), and the pure Pt(111) slab, respectively.

First, in order to look into how the TM sublayer affects the surface-states, we examined valence band structure projected on surface-states. **Figure 3**a and Figure 3b show the band structures of Pt-Ni(111) surface that are color-coded according to the weight on surface Pt and subsurface Ni atoms, respectively. It is seen that the surface Pt layer on $Pt_3Ni(111)$ has a relatively weak character of surface-states in comparison with that on Pt(111).[22] In contrast, Ni atom in the subsurface layer results in strong surface electronic structure near the Fermi level as shown in Figure 3b.

To map out the influence of subsurface Ni more clearly, the partial DOS (PDOS) for *s*, $d_{xz,yz}$, d_{xy}, and d_{z^2} of Pt(111) and Pt-Ni(111) are compared in Figure 3c and Figure 3d. Comparing two PDOSs, it is seen that the *d* bands of the surface Pt layer on Pt-Ni(111) overall shift down when compared to that on Pt(111), resulting in the reduced contribution of surface *d* bands near the Fermi level, particularly $d_{xz,yz}$ states, which are key states involved in chemical bonding with atomic oxygen. In contrast, the Ni *d* bands in the subsurface layer have a pronounced weight near the Fermi level, consistent with the band-structure analysis in the above. The shift-down of surface *d* bands can be explained based on the induced charge polarization between surface and subsurface layers.[25]

To verify the charge polarization on the Pt surface and Ni subsurface layer, Bader charge analysis was performed. The reference values of Bader charge were set to those for the unrelaxed, bulk-terminated Pt(111) surface. The charge redistribution of Pt(111) after interlayer relaxation is negligible: surface = +0.05, subsurface = –0.04, 3rd-layer = –0.02, and 4th-lyaer = +0.01 (here, the negative sign means that electrons are depleted on that layer). On the other hand, the presence of Ni atoms in the subsurface layer, i.e., Pt-Ni(111), gives rise to substantial changes of local charge distribution: surface = +0.23, subsurface = –0.42, 3rd-layer = +0.17, and 4th-lyaer = +0.02 (see Supporting information, Table S1,S2). The significant amount of charge redistribution at the surface and subsurface layer (i.e., charge polarization) causes a variation of the interlayer potential resulting in downshift of Pt surface bands. These results and analysis are consistent with the above-mentioned core-level shift of 0.15 eV for Pt surface layer in Figure 1b. Since the surface-states near the Fermi level is mainly responsible for the Pt-O bonding, the suppression of these states near the Fermi level by the modified potential can account for their weak oxygen adsorption properties.

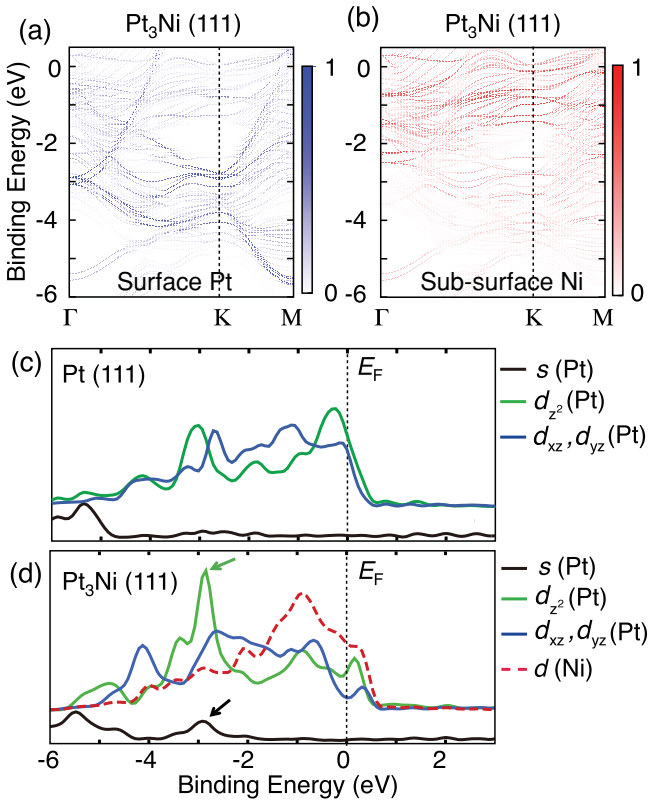

Figure 3. Surface band structures a) at Pt surface layer and b) at Ni sub-surface layer, respectively. The Pt surface layer shows very weak surface-states while the Ni sub-surface layer shows strong weights near the Fermi level. c,d) Partial density of state (PDOS) for *s*, $d_{xz,yz}$, d_{xy}, and d_{z^2} of Pt(111) and Pt-Ni(111), respectively. PDOS of Pt-Ni(111) alloy shows hybridization between *s* and d_{z^2} resulting from the significant potential change caused by the charge polarization between top and subsurface layer.

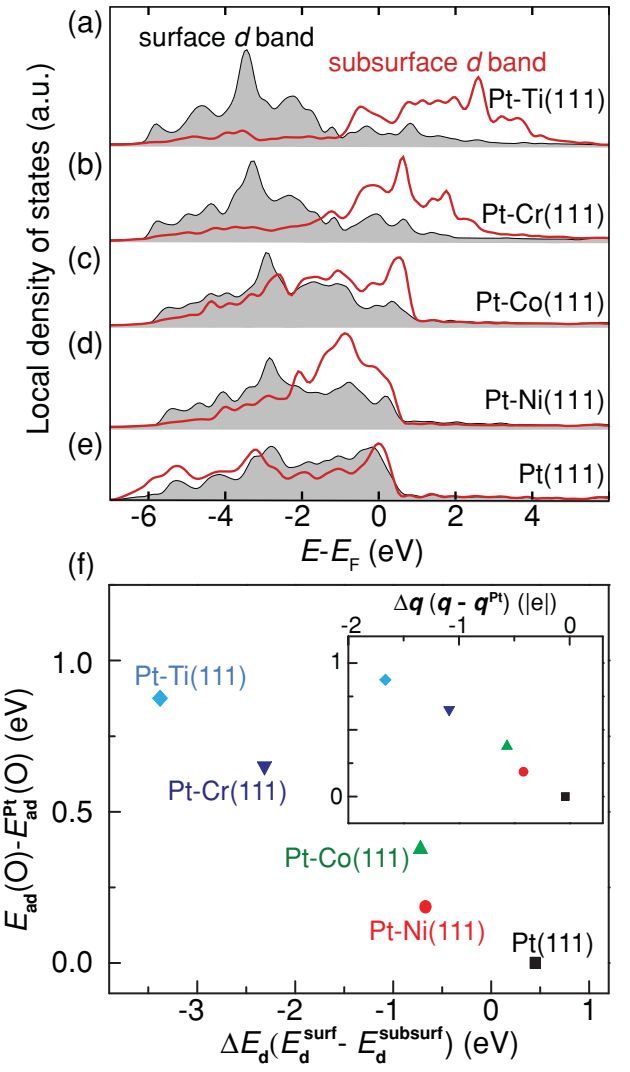

Figure 4. a–e) The *d* band local DOS (LDOS) for surface and subsurface layer of Pt(111) and Pt-TM(111). f) Oxygen adsorption energy on the Pt(111) and Pt-TM(111) surfaces as a function of the difference in center LDOS distribution between surface and subsurface layer. Inset shows the Bader change of Pt-surface layer on the Pt-TM(111) relative to that on Pt(111) ($\Delta q = q - q^{Pt}$).

To confirm the charge polarization effect due to the alloyed TM atoms, we extended the calculations to other Pt-TM alloy systems. **Figure 4**a–e presents the calculated *d* band local DOS (LDOS) for surface and subsurface layer of Pt(111) and Pt-TM(111). In Figure 4a–e, it is clearly seen that (1) the overall downshift of *d* band LDOSs of Pt surface layer and (2) the enhancement of *d*-band weight of TM near the Fermi level. To be consistent with ARPES results, the *d*-band LDOSs for surface layer of Pt-Ni and Pt-Co(111) overall shift down, resulting in suppression of surface-states near the Fermi level, while that for Ni(Co)-subsurface layer is enhanced near the Fermi level (Figure 4c and d). The difference of LDOS distribution around the Fermi level between surface and subsurface layer gradually increases from Pt-Ni(111) to Pt-Ti(111).

To see the correlation between the degrees of surface polarization and oxygen adsorption energy, we calculated how oxygen adsorption energies depend on the charge polarization on each Pt-TM(111) surfaces. Figure 4f shows oxygen adsorption energy on the Pt(111) and Pt-TM(111) surfaces as a function of the difference in the LDOS center between surface (E_d^{surf}) and subsurface layers ($E_d^{subsurf}$), which represents the charge polarization. The inset of Figure 4f displays how the oxygen adsorption energy depends on the Bader charge of Pt-surface layer evaluated with respect to the pure Pt(111) surface ($\Delta q = q - q^{Pt}$). The linear relationship supports that the oxygen adsorption is weakened as the charge polarization is enhanced.

In summary, we demonstrated that TM atoms in the subsurface layer soften the chemical bonding between Pt and adsorbed atomic oxygen due to the suppression of surface-states on the Pt surface layer. Modified surface-state of Pt surface layer is the key component that affects chemical bonding between oxygen atom and $Pt_3TM(111)$ surface. The TM atoms in the subsurface layer induce charge redistribution between Pt-surface and TM-subsurface layer resulting in different interlayer potential,

i.e. charge polarization, and suppression of surface-state. By showing that the degree of charge polarization plays an important role in modifying chemical reactivity of surface, we believe that the present results provide a deeper understanding on how the surface electronic structures can be altered by the subsurface potentials in metal alloy systems.

Experimental Section

Sample preparation: A clean Pt(111) and $Pt_3TM(111)$ (TM = Ni, Co) surfaces, showing a well-ordered (1 × 1), were carefully prepared by repeated sputtering and annealing. No carbon or O contamination was detected on the prepared surface by X-ray photoemission spectroscopy.

HR-XPS and ARPES measurements: The core-level HR-XPS and ARPES measurements were performed at beamline 7.0.1 of the Advanced Light Source. The ARPES band structures were measured by the photon energy of 120 eV. The ARPES map along *k* (surface normal) were collected by scanning the photon energy from 100 to 160 eV.

DFT calculations: The cut-off energy for the plane-wave basis is set to 400 eV. For *k*-point sampling, 14 × 14 × 1 meshes are used for the slab structure and all atoms were allowed to relax until the Hellmann–Feynman force on them become less than 0.03 eV/Å.

Supporting Information

Supporting Information is available from the Wiley Online Library or from the author.

Acknowledgements

Y.S.K. and S.H.J. contributed equally to this work. Y.S.K. was supported by the Institute of Basic Science (IBS) (EM1203). B.S.M. would like to thank the support by Basic Science Research Program through the National Research Foundation of Korea (NRF) by the Ministry of Education, Science and Technology (MEST) (2012R1A1A2001745). Also, this work and ALS were supported by the U.S. Depart-ment of Energy, Office of Basic Sciences under Contract No. DE-AC02-05CH11231. S.H.J. and S.W. were supported by the Center for Multiscale Energy System. The first-principles computations were carried out at KISTI (KSC-2012-C3-08). This paper was supported by GIST College's 2013 GUP Research Fund.

Received: February 14, 2013
Revised: April 8, 2013
Published online: May 29, 2013

[1] R. Hoffmann, *Rev. Mod. Phys.* **1998**, *60*, 601.
[2] B. L. M. Hendriksen, J. W. M. Frenken, *Phys. Rev. Lett.* **2002**, *89*, 046101.
[3] X.-Q. Gong, Z.-P. Liu, R. Raval, P. Hu, *J. Am. Chem. Soc.* **2004**, *126*, 8.
[4] M. D. Ackermann, T. M. Pedersen, B. L. M. Hendriksen, O. Robach, S. C. Bobaru, I. Popa, C. Quiros, H. Kim, B. Hammer, S. Ferrer, J. W. M. Frenken, *Phys. Rev. Lett.* **2005**, *95*, 255505.
[5] R. B. Getman, W. F. Schneider, A. D. Smeltz, W. N. Delgass, F. H. Ribeiro, *Phys. Rev. Lett.* **2009**, *102*, 076101.
[6] E. M. Larsson, C. Langhammer, I. Zoric, B. Kasemo, *Science* **2009**, *326*, 1091.
[7] A. D. Smeltz, R. B. Getman, W. F. Schneider, F. H. Ribeiro, *Catal. Today* **2004**, *136*, 84.
[8] D. Strmcnik, K. Kodama, D. van der Vliet, J. Greeley, V. R. Stamenkovic, N. M. Markovic, *Nat. Chem.* **2009**, *1*, 466.
[9] L. Qi, X. Qian, J. Li, *Phys. Rev. Lett.* **2008**, *101*, 146101.
[10] H. A. Gasteiger, S. S. Kocha, B. Sompalli, F. T. Wagner, *Appl. Catal. B* **2005**, *56*, 9.
[11] J. Greeley, I. E. L. Stephens, A. S. Bondarenko, T. P. Johansson, H. A. Hansen, T. F. Jaramillo, J. Rossmeisl, I. Chorkendorff, J. K. Nørskov, *Nat. Chem.* **2009**, *1*, 552.
[12] V. R. Stamenkovic, B. Fowler, B. S. Mun, G. Wang, P. N. Ross, C. A. Lucas, N. M. Markovic, *Science* **2007**, *315*, 493.
[13] V. R. Stamenkovic, B. S. Mun, M. Arenz, K. J. J. Mayrhofer, C. A. Lucas, G. Wang, P. N. Ross, N. M. Markovic, *Nat. Mat.* **2007**, *6*, 241.
[14] J. K. Nørskov, T. Bligaard, J. Rossmeisl, C. H. Christensen, *Nature Chem.* **2009**, *1*, 37.
[15] The *d*-band model conceptually follows the Sabatier's principle; P. Sabatier, *Ber. Deutsch. Chem. Gesellshaft* **1911**, *44*, 1984; moderate bonding strength (cohesion energy), neither too strong nor too weak, leading to the highest electrocatalytic reaction.
[16] B. Hammer, J. K. NørsKov, *Nature* **1995**, *376*, 238.
[17] V. Stamenkovic, B. S. Mun, K. J. J. Mayrhofer, P. N. Ross, N. M. Markovic, J. Rossmeisl, J. Greeley, J. K. Nørskov, *Angew. Chem.* **2006**, *118*, 2963.
[18] K. Gustafsson, S. Andersson, *Phys. Rev. Lett.* **2006**, *97*, 076101.
[19] Y. S. Kim, A. Bostwick, E. Rotenberg, P. N. Ross, S. C. Hong, B. S. Mun, *J. Chem. Phys.* **2010**, *133*, 034501.
[20] A. Gross, In *The Chemical Physics of Solid Surfaces*, *Vol. 11* (Ed. D.P. Woodruff), Elsevier, USA **2003**, Ch. 1, pp 1–26.
[21] A. Groβ, A. Eichler, J. Hafner, M. J. Mehl, D. A. Papaconstantopoulos, *Surf. Sci.* **2003**, *539*, L542.
[22] Y. S. Kim, S. H. Jeon, A. Bostwick, E. Rotenberg, P. N. Ross, A. L. Walter, Y. J. Chang, V. R. Stamenkovic, N. M. Markovic, T. W. Noh, S. Han, B. S. *Mun, Phys. Chem. Chem. Phys*. in press.
[23] P. E. Blochl, *Phys. Rev. B* **1994**, *50*, 17953.
[24] J. P. Perdew, K. Burke, M. Ernzerhof, *Phys. Rev. Lett.* **1996**, *77*, 3865.
[25] R. Wu, A. J. Freeman, *Phys. Rev, B* **1995**, *52*, 12419.